

Sensitivity performance of Ag/TiN and Ag/ZrN based SPR sensors for glucose and sucrose identification

WAN MAISARAH MUKHTAR*, NURUL ATIRAH NURADDIN

Faculty of Science and Technology, Universiti Sains Islam Malaysia (USIM), Bandar Baru Nilai, 71800 Nilai, Negeri Sembilan, Malaysia

This study was carried out to investigate the effect of hybrid plasmonic material thicknesses, which are Ag/TiN and Ag/ZrN on the sensitivity of SPR sensor in detecting glucose and sucrose. A Krestchmann configuration of surface plasmon resonance (SPR) sensor had been theoretically developed via prism coupling technique. A 633nm of red laser was incident onto the prism's hypotenuse side to excite the SPR. The effect of Ag/TiN and Ag/ZrN thicknesses ranging from 35nm to 60nm on the sensitivity of SPR sensor was studied. The deployment of Ag/ZrN at 44nm/10nm thicknesses resulted the resonance angle shifting about 0.91° from 44.67° to 45.58° as it was exposed to the glucose and sucrose. In contrary, the Ag/TiN coated sensor indicated large angle shifting only for glucose detection which portrays its non-versatility feature. The proposed Ag/ZrN based SPR sensor able to identify the analytes, with almost similar refractive index values with sensitivity values of 0.6725 °/RIU (glucose detection) and 0.6724°/RIU (sucrose detection). In conclusion, Ag/ZrN ($t_{Ag}=44\text{nm}$, $t_{ZrN}=10\text{nm}$) offers better sensitivity and selectivity performance than Ag/TiN because of the absorption enhancement inside the Ag due to the high scattering efficiency of ZrN.

(Received May 12, 2021; accepted November 24, 2021)

Keywords: Surface plasmon resonance (SPR), Silver/Titanium Nitrate (Ag/TiN), Silver/Zirconium Nitrate (Ag/ZrN), Glucose, Sucrose, Honey

1. Introduction

Honey is a complex, natural food with a lot of benefits for humans [1]. It consists of various chemical components, and carbohydrates are the main components, including glucose, sucrose and fructose [2]. The quality standard for honey has been introduced by the international standardization organization such as Gulf Standardization Organization (GSO). According to GSO standard, the specification of honey composition such as fructose, glucose and sucrose should be within 27% to 44.3%, 22% to 40.7% and less than 5% respectively [3]. The biochemical variation in the composition of pure honey can ensure the taste and benefits of originality [4].

Electronic sensing technique such as electronic nose (e-nose) and electronic tongue (e-tongue) have been used to identify adulterated honey [5,6]. Recently, optical sensors also have been used in food safety area to detect the quality of food including honey [7-9]. The optical sensors exhibit excellent sensitivity down to nanoscale detection since their main operating principle rely on photon propagation. In general, optical sensors can be divided into two categories which are fiber optics sensor [10-13] and free space optics sensor such as prism-based sensor and silicon-based sensor [14,15].

Surface plasmon resonance (SPR) is a phenomenon which is created as a p-polarized light incident on noble metal. Since SPR is a non-destructive process, it is appropriate for various applications in the fields of biology

and chemistry [16-19]. This optical method does not influence the substance's composition and it is favorable for natural composition sensing, such as liquid honey [20].

Noble metal is one of the important requirements to generate SPR. Gold (Au) offers a good chemical stability [21, 22]. The disadvantage of this metal is due to its broader resonance curves that limit the accuracy of detection. In contrast, the silver has sharp resonance peak that achieves higher detection accuracy [23]. However, silver suffers greatly from oxidation. An additional protective layer such as TiO₂ (titanium dioxide) and GO (graphene oxide) is required to prevent this problem [24, 25]. Recently, the transition metal nitrides such as titanium nitride (TiN) and zirconium nitride (ZrN) become favorable materials for plasmonic applications in visible and near infrared region due to their tailorable optical properties and refractory quality [26, 27]. These materials exhibit a very high melting point, high chemical stability, and excellent ruggedness. Such properties make TiN and ZrN perfect candidates as a coating layer material for the SPR sensor.

This work aims to investigate the effect of hybrid plasmonic materials' thicknesses, which are Ag/TiN and Ag/ZrN on the sensitivity of SPR sensor in detecting glucose and sucrose. The total films thicknesses are varied between 35 nm to 60 nm to determine the optimized physical properties of the material for the development of high sensitivity SPR sensor. The output of this study found that the deployment of Ag/ZrN at thicknesses of 44 nm/10

nm exhibits better sensitivity than Ag/TiN because of the absorption enhancement inside the Ag due to the high scattering efficiency of ZrN. We believe that the proposed sensor will have a good future in food safety area, specifically for adulterated honey detection due to its versatility in identifying the presence of glucose and sucrose.

2. Materials and methods

WinSpall 3.02 simulation software based on Fresnel equation was used to study the sensitivity of our proposed SPR sensor. Fig. 1 illustrates the setup of this work. SPR was created by employing Kretschmann configuration coupling technique. A p-polarized Helium Neon (He-Ne)

laser with operating wavelength of 633 nm was incident through the prism onto its hypotenuse side. The hypotenuse side of the prism was coated with two nanolayers of materials, namely silver/titanium nitrate (Ag/TiN) and silver/zirconium nitrate (Ag/ZrN). The thicknesses of Ag were varied between 30 nm to 50 nm, meanwhile for ZrN and TiN, their thicknesses were controlled between 5 nm to 10 nm. The SPR phenomena was created by controlling the light incident angle from 38° to 58° with an increment of 0.30° per reading. The physical and optical properties of the materials are listed in Table 1. The characteristics of the resulting SPR curves, such as minimum reflectance value (R_{\min}), sensor's sensitivity and amount of angle shifting had been investigated.

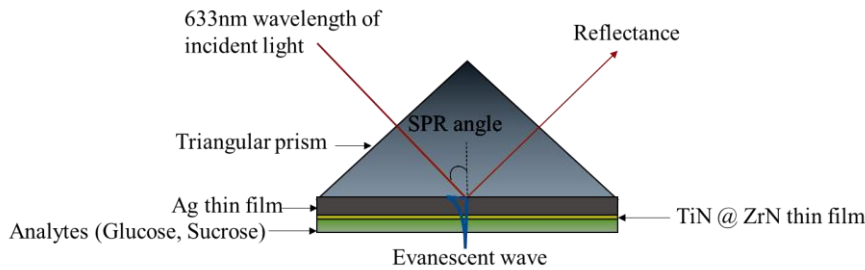


Fig. 1. Detection of sugar classification using SPR sensor (color online)

Table 1. List of materials and their parameters

Material	Thickness, t (nm)	Refractive index, RI (a.u)
Glass prism	-	1.51
Silver (Ag)	30-50	0.13511, 3.9852
Zirconium nitrate (ZrN)	5, 7, 10	1.34, 0.9852 [28]
Titanium nitrate (TiN)	5, 7, 10	1.3512, 2.7599 [28]
Glucose	-	1.3532, 0.0002 [29]
Sucrose	-	1.3533, 0.0002 [30]

3. Results and discussions

Fig. 2(a) displays the characteristics of SPR curves when various thicknesses of hybrid layers of Ag (30 nm to 50 nm) and ZrN (5 nm, 7 nm and 10 nm) were deposited on the hypotenuse side of the triangular glass prism. Note that, the strength of SPR signal can be evaluated based on the SPR curve depth, or usually is called as Q-factor [31]. Obviously, as the thicknesses of ZrN increased from 5 nm to 10 nm, the Q-factor started to decrease which explain the optimum thickness of ZrN for maximum generation of SPR due to greater amount of surface plasmon polaritons excitation [19]. The increment of SPR curve's width (full-width-half-maximum (FWHM)) with the increased of ZrN thicknesses proves that the additional

layer on top of metal (Ag) must be controlled at a very thin thickness. In SPR, small value of FWHM is favorable since it exhibits the capability of sensor in detecting small changes of the analyte's refractive index [23]. At $t_{\text{ZrN}} = 5$ nm, the smallest R_{\min} value about 0.0021 a.u had been obtained with thickness of Ag was 30 nm. When $t_{\text{ZrN}} = 7$ nm, minimum value of R_{\min} was observed at $t_{\text{Ag}} = 30$ nm with $R_{\min} = 0.0204$ a.u. The smallest R_{\min} value at $t_{\text{ZrN}} = 10$ nm was resulted as 0.0791 a.u had been recorded by setting the thickness of Ag at 30 nm. Apparently, maximum SPR signal was successfully generated by sustained the thickness of Ag at 30 nm. Note that the SPR generation is mainly influenced by metal thicknesses. If the metal is too thin, the surface plasmon polaritons (SPP) will be strongly damped because of radiation damping into prism. If the metal is too thick, the SPP can no be longer efficiently excited due to absorption in the metal. The position of SPR dip in the reflectance curves can be used as an indicator for the environmental changes detection, in which in this study it refers to the presence of glucose and sucrose [32]. As the coating material was replaced with TiN (Fig. 2(b)), value of R_{\min} increased about 13.58% with $R_{\min} = 0.0134$ a.u at $t_{\text{TiN}} = 5$ nm and $t_{\text{Ag}} = 30$ nm. When thickness of TiN increased to 7 nm, value of R_{\min} was obtained as 0.0693 a.u. Meanwhile, the lowest R_{\min} value at 0.1796 a.u was resulted when $t_{\text{TiN}} = 10$ nm. The SPR angles were found to be red-shifted from 43.16° to 44.07° as thicknesses for both hybrid layers (Ag/TiN and Ag/ZrN) increased.

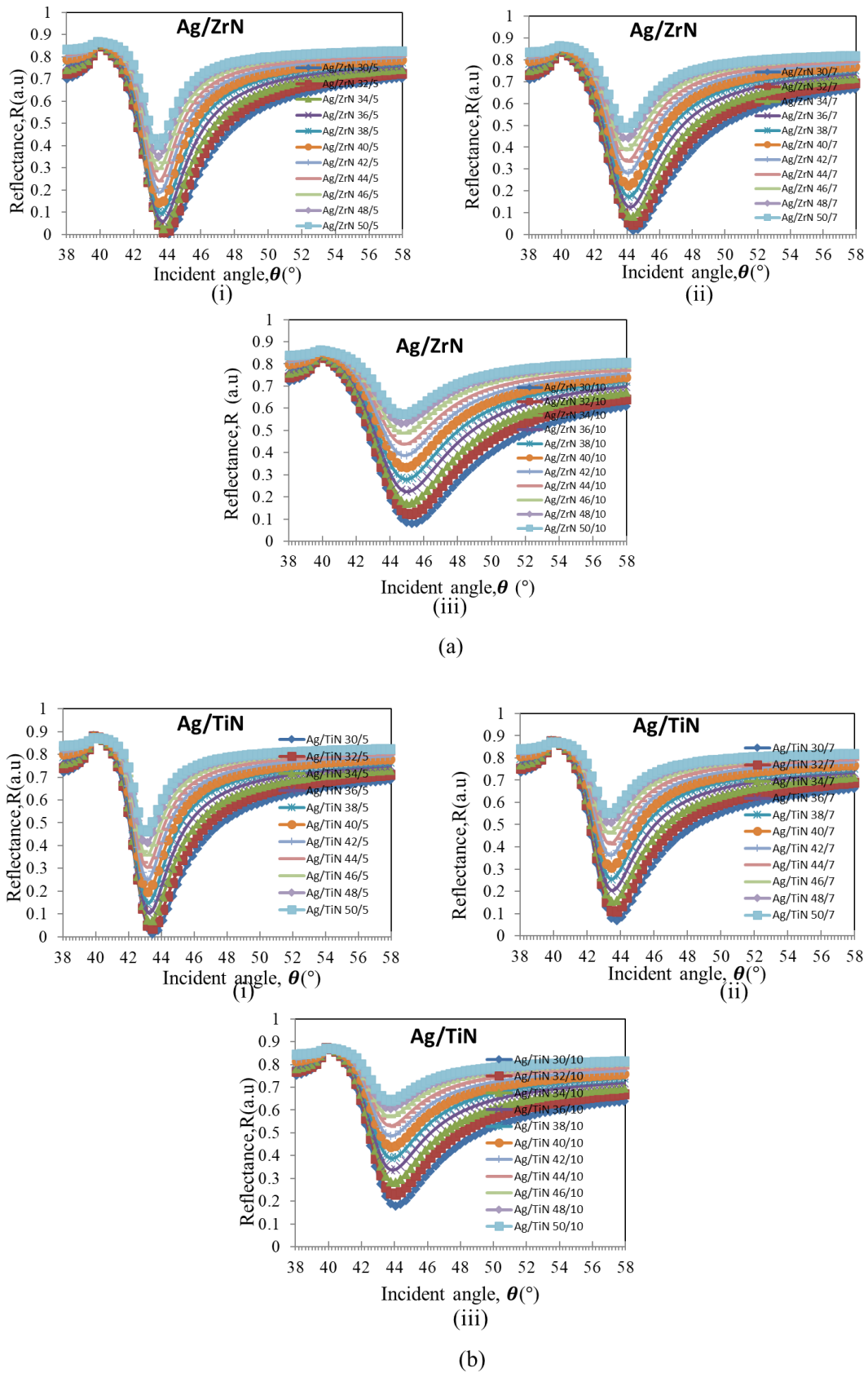
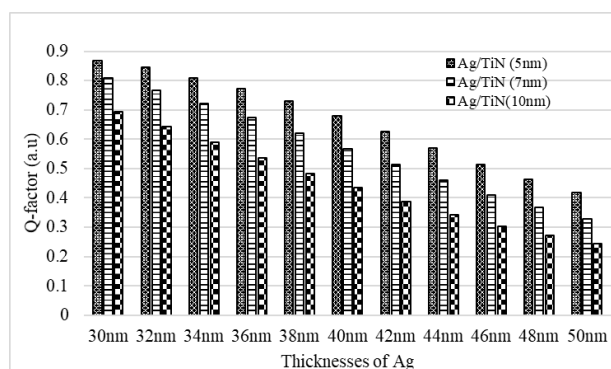


Fig. 2. Effect of material's thicknesses on SPR signal (a) Ag/ZrN ($t_{Ag} = 30\text{ nm}-50\text{ nm}$, (i) $t_{ZrN} = 5\text{ nm}$, (ii) 7 nm (iii) 10 nm)
 (b) Ag/TiN ($t_{Ag} = 30\text{ nm}-50\text{ nm}$, (i) $t_{TiN} = 5\text{ nm}$, (ii) 7 nm (iii) 10 nm) (color online)

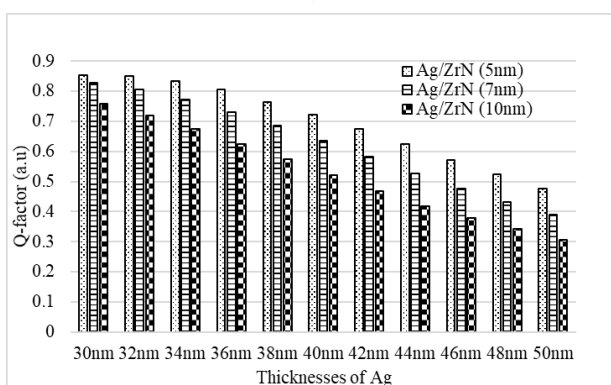
Fig. 3 displays the Q-factor analyses of SPR curves for Ag/TiN (Fig. 3(a)) and Ag/ZrN (Fig. 3(b)). Obviously, large Q-factor values were obtained as the additional layer of TiN or ZrN with both thicknesses at 5 nm were coated on Ag thin film due to their low loss and excellent metallic properties [29]. As the Ag thin film thicknesses increased from 30 nm to 50 nm, values of Q-factor decreased linearly which suggest the generation of strong SPR signal at minimum thickness. Fig. 4 shows the Q-factor comparison between both materials at their optimized total thicknesses, $t = 35$ nm ($t_{Ag} = 30$ nm and $t_{ZrN}@t_{TiN} = 5$ nm). The deployment of Ag/ZrN resulted greater Q-factor value than Ag/TiN with maximum differences up to 13.46%. It can be concluded that strong SPR signal was successfully generated by employing Ag/ZrN with total thicknesses of 35 nm owing to their non-stoichiometric compositions. This drastic change in film properties can be useful in building plasmonic devices where the properties of the material components need to be tuned or graded [28].

Fig. 5 exhibits various SPR curves of Ag/TiN based sensor for detection of sucrose (Fig. 5(a)) and glucose (Fig. 5(b)). In general, angle shifting had been occurred at all thicknesses of Ag/TiN and Ag/ZrN as they exposed to the analytes. At certain thicknesses, large angle shifting had been recorded which reflects the ability of these hybrid materials to detect the presence of analytes. Apparently, the Ag/TiN sensor indicated the greatest SPR curve depth and obvious angle shifting when $t_{TiN} = 5$ nm as illustrates in Fig. 5(a)(i) and Fig. 5(b)(i).

Similar analyses had been performed on the Ag/ZrN coated SPR sensor as depicted in Fig. 6. In general, the maximum Q-factor values were obtained as thicknesses of Ag were set within 36 nm to 42 nm. The apparent SPR angle shifting was observed as the analytes were switched from sucrose (Fig. 6(a)) to glucose (Fig. 6(b)) at $t_{ZrN} = 10$ nm. It was found that the deployment of Ag/ZrN at thicknesses of $t_{Ag} = 44$ nm and $t_{ZrN} = 10$ nm resulted greatest amount of angle shifting which is 0.91° from 44.67° to 45.58° (Fig. 7(a) and Fig. 7(b)). It is noteworthy to mention that similar amount of angle shifting for both analytes owing to the value of refractive index of sucrose and glucose which are almost equal with difference between them is only about 0.0001 a.u.



(a)



(b)

Fig. 3. Analyses of Q-factor values of SPR curves (a) Ag/TiN (b) Ag/ZrN

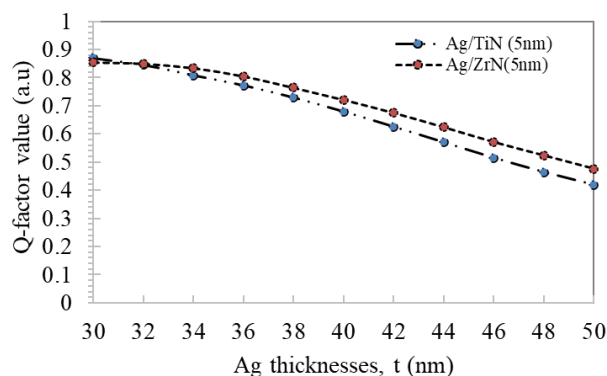


Fig. 4. Q-factor values of SPR curves for Ag/TiN and Ag/ZrN with total thickness of 35 nm ($t_{Ag} = 30$ nm and $t_{ZrN}@t_{TiN} = 5$ nm) (color online)

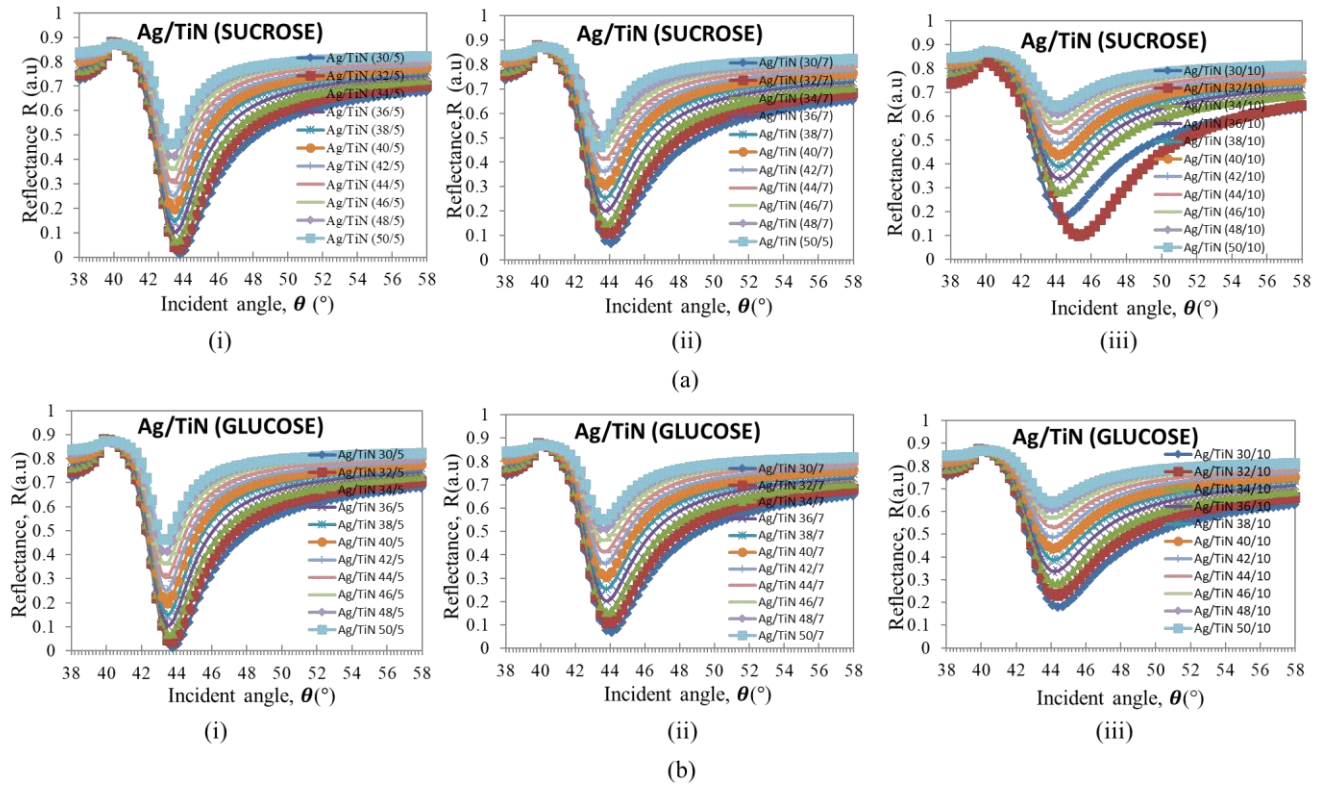


Fig. 5. SPR curves as the Ag/TiN SPR sensor exposed to the two types of sugar (a) sucrose detection ($t_{Ag} = 30 \text{ nm}-50 \text{ nm}$, (i) $t_{TiN} = 5 \text{ nm}$, (ii) $t_{TiN} = 7 \text{ nm}$ (iii) $t_{TiN} = 10 \text{ nm}$) (b) glucose detection ($t_{Ag} = 30 \text{ nm}-50 \text{ nm}$, (i) $t_{TiN} = 5 \text{ nm}$ (ii) $t_{TiN} = 7 \text{ nm}$ (iii) $t_{TiN} = 10 \text{ nm}$) (color online)

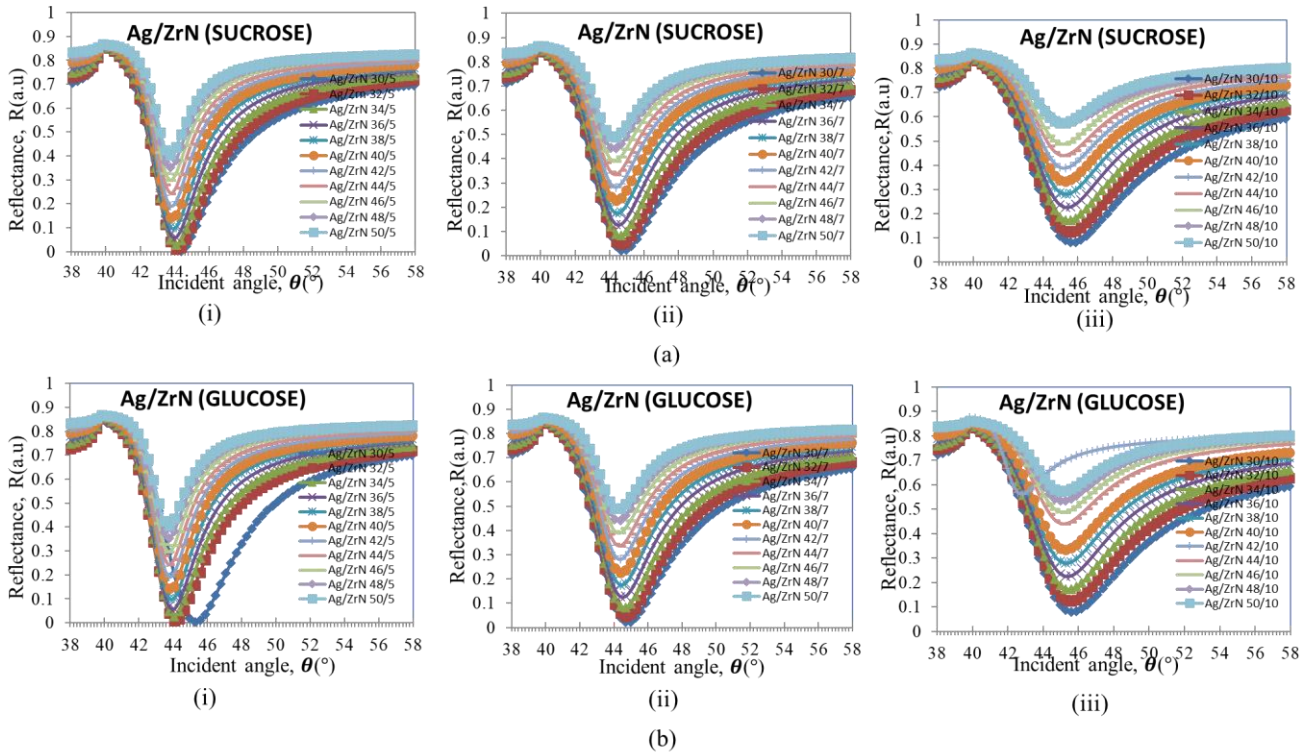


Fig. 6. SPR curves as the Ag/ZrN SPR sensor exposed to the two types of sugar (a) sucrose detection ($t_{Ag} = 30 \text{ nm}-50 \text{ nm}$, (i) $t_{ZrN} = 5 \text{ nm}$, (ii) $t_{ZrN} = 7 \text{ nm}$ (iii) $t_{ZrN} = 10 \text{ nm}$) (b) glucose detection ($t_{Ag} = 30 \text{ nm}-50 \text{ nm}$, (i) $t_{ZrN} = 5 \text{ nm}$, (ii) $t_{ZrN} = 7 \text{ nm}$ (iii) $t_{ZrN} = 10 \text{ nm}$) (color online)

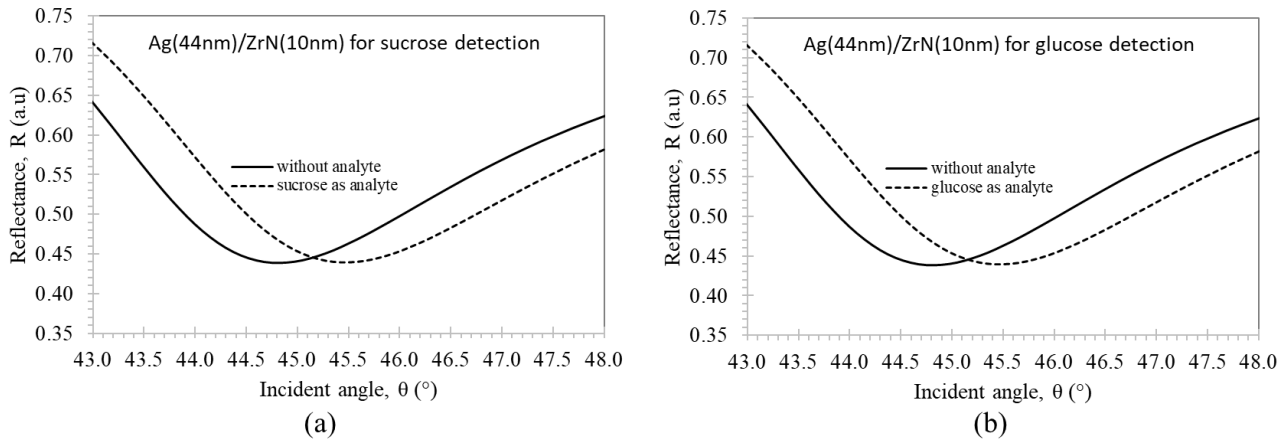


Fig. 7. Maximum SPR angle shifting as the Ag(44 nm)/ZrN(10 nm) SPR sensor (a) sucrose detection (b) glucose detection

At thicknesses of $t_{Ag} = 34$ nm and $t_{ZrN} = 10$ nm, the amount of angle shifting was obtained as 0.61° (Fig. 8). In comparison with $Ag_{t=44nm}/ZrN_{t=10nm}$ based SPR sensor, the amount of shifting decreased about 32.97%. The usage of $Ag_{t=32nm}/TiN_{t=10nm}$ resulted the maximum angle shifting which is about 1.20° as illustrated in Fig. 9. Unfortunately, this configuration did not show similar characteristics for glucose sensing (refer Fig. 2(b) and Fig. 5(b)). This output indicates the nonversatility of Ag/TiN based SPR sensor in classifying various types of sugar. Except $Ag_{t=44nm}/ZrN_{t=10nm}$, the remain thicknesses of Ag/ZrN portray small angle shifting about 0.61° as exposed to the analytes. Fig. 10 exhibits the example of SPR angle shifting before and after the sensor reacted with the analytes. In general, the sensor fabricated by Ag/ZrN and Ag/TiN with various thicknesses able to detect the

presence of glucose and sucrose. But, the maximum sensitivity with consistent detection was successfully obtained by using Ag/ZrN with $t_{Ag} = 44$ nm and $t_{ZrN} = 10$ nm.

In comparison with a single gold coated SPR sensor, our proposed Ag/ZrN based sensor offers 1.67% better sensitivity in detecting sucrose and glucose [3]. In addition, few outstanding features of TiN and ZrN such as able to stand at very high melting point, have high chemical stability and excellent ruggedness make them extraordinary sensing materials. Compare with another design of sensor such as an optical chiral sensor using optical weak measurement system, our sensor experiences greater shifting of response curve about 33.33% which indicates its excellent sensitivity feature as exposed to the analytes [33].

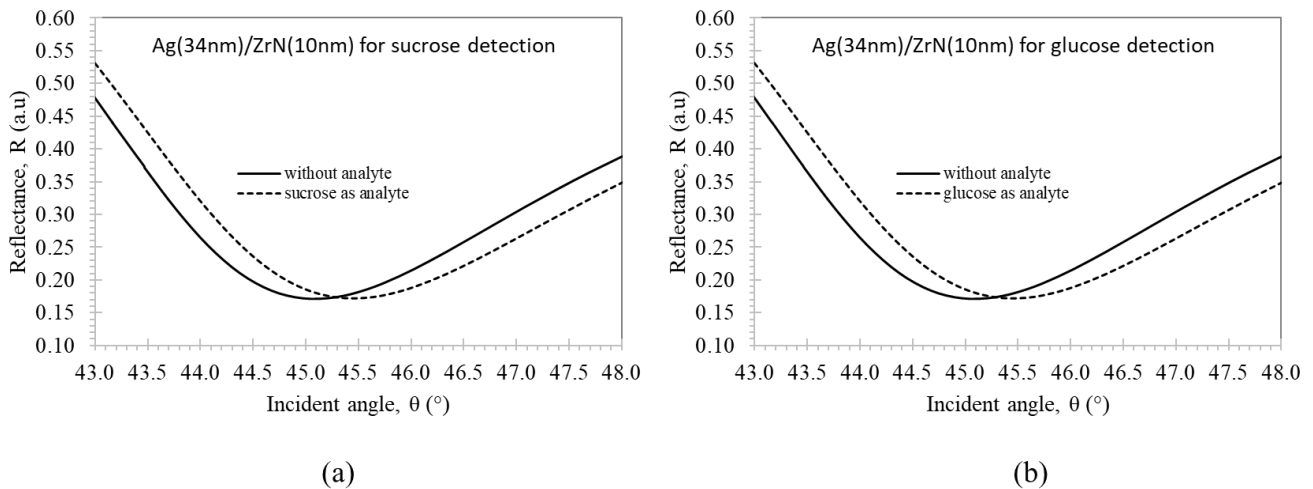


Fig. 8. Maximum SPR angle shifting using Ag(34 nm)/ZrN(10 nm) based SPR sensor (a) sucrose detection (b) glucose detection

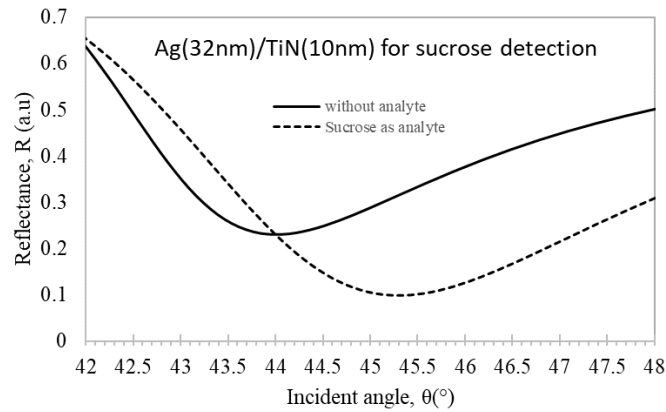


Fig. 9. Maximum SPR angle shifting using Ag(32 nm)/TiN(10 nm) based SPR sensor for sucrose detection

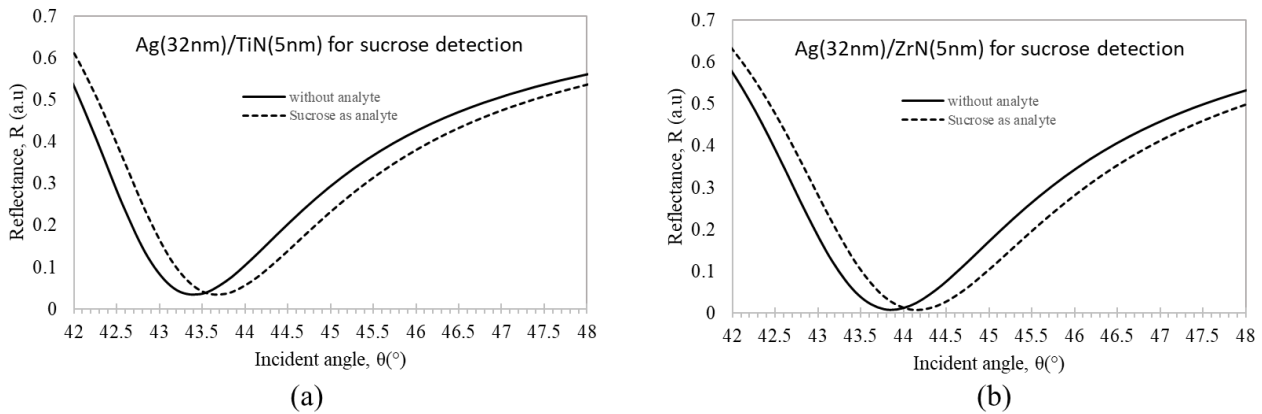


Fig. 10. Similar SPR angle shifting for sucrose detection using different materials at certain thicknesses (a) Ag/TiN (b) Ag/ZrN

Table 2. Sensitivity analysis of SPR sensor

Material	Thicknesses	Sensitivity, S (%/RIU)	
		Glucose	Sucrose
Ag/ZrN	44nm/10nm	0.6725	0.6724
Ag/ZrN	34nm/10nm	0.4508	0.4508
Ag/ZrN and Ag/TiN	Other thicknesses	0.2217	0.2217

Table 2 shows the sensitivity analyses of SPR sensor using various types and thicknesses of materials. Obviously, the usage of Ag/ZrN hybrid plasmonic materials at thicknesses of $t_{Ag} = 44$ nm and $t_{ZrN} = 10$ nm offer the best sensitivity which are 0.6725 %/RIU and 0.6724 %/RIU for sucrose and glucose sensing, respectively. Small sensitivity differences between both sensing materials owing to their refractive index values which are nearly the same. At thicknesses of $t_{Ag} = 34$ nm and $t_{ZrN} = 10$ nm, lower sensitivity value 0.4508 %/RIU had been obtained for both analytes detection. Meanwhile, at

other thicknesses, the Ag/ZrN and Ag/TiN based SPR sensors exhibits low sensitivity about 0.2217 %/RIU. Overall, the Ag/ZrN ($t_{Ag} = 44$ nm, $t_{ZrN} = 10$ nm) offers the best sensitivity and selectivity performance due to its low loss and high metallic properties. The presence of a very thin layer of ZrN obviously enhanced the sensitivity of the SPR sensor because of the absorption enhancement inside the Ag due to the high scattering efficiency of ZrN [34].

4. Conclusions

The transition metal nitrides such as titanium nitride (TiN) and zirconium nitride (ZrN) exhibits excellent sensing properties for plasmonic applications in visible and near infrared region due to their tailorable optical properties and refractory quality. The performance analyses between these materials indicate that hybrid thin films Ag/ZrN at thicknesses of 44 nm/10 nm results the best sensitivity for glucose and sucrose detection. The proposed Ag/ZrN based SPR sensor able to identify the analytes, with almost similar refractive index values. For future work, the effect of light intensity and types of prism

configurations on the sensitivity of Ag/ZrN based SPR sensor for adulterated honey detection will be investigated.

Acknowledgement

We would like to thank the Knoll Group from Max Plank Institute for the Winspall 3.02 simulation software. The Faculty of Science and Technology (FST), USIM is also acknowledged for the research facilities.

References

- [1] G. Dolezal, A. L. Toth, *Curr. Opin. Insect. Sci.* **26**, 114 (2018).
- [2] N. M. Razali, A. N. Mazlan, M. F. Salebi, H. Mohamed, S. Ambran, *Telkomnika (Telecommunication Comput. Electron. Control)* **17**, 2445 (2019).
- [3] B. A. Alghamdi, E. S. Alshumrani, M. S. B. Saeed, G. M. Rawas, N. T. Alharthi, M. N. Baeshen, et al., *Saudi J. Biol. Sci.* **27**, 3720 (2020).
- [4] N. H. Zainuddin, Y. W. Fen, A. A. Alwahib, M. H. Yaacob, N. Bidin, N. A. S. Omar, M. A. Mahdi, *Optik* **168**, 134 (2018).
- [5] S. Faal, M. Loghavi, S. Kamgar, *Measurement* **148**, 106936 (2019).
- [6] M. Oroian, S. Paduret, S. Ropciuc, *J. Sci. Food Agric.* **98**, 4304 (2018).
- [7] W. M. Mukhtar, I. Kamarolzaman, *Journal of Mechanical Engineering and Sciences* **14**, 7540 (2020).
- [8] N. Irawati, N. M. Isa, A. F. Mohamed, H. A. Rahman, S. W. Harun, H. Ahmad, *IEEE Sens. J.* **17**, 5510 (2017).
- [9] W. M. Mukhtar, N. H. M. K. Pang, R. M. Halim, In *Nano Hybrids and Composites.*, Trans. Tech. Publications Ltd **31**, 45 (2021).
- [10] Q. Yao, G. Ren, K. Xu, L. Zhu, H. Khan, M. Mohiuddin, M. W. Khan, B. Y. Zhang, A. Jannat, F. Haque, S. Z. Reza, Y. Wang, X. Wen, A. Mitchell, J. Z. Ou, *Adv. Opt. Mater.* **7**, 1901383 (2019).
- [11] A. H. Kamarulzaman, W. M. Mukhtar, *Science Letters* **14**, 1 (2020).
- [12] W. M. Mukhtar, S. N. Latib, R. M. Halim, A. R. A. Rashid, In *Solid State Phenomena Trans. Tech. Publications Ltd* **307**, 78 (2020).
- [13] N. Bidin, N. H. Zainuddin, S. Islam, M. Abdullah, F. M. Marsin, M. Yasin, *IEEE Sens. J.* **16**, 299 (2015).
- [14] W. M. Mukhtar, R. M. Halim, H. Hassan, In *EPJ Web of Conferences EDP Sciences* **162**, 01001 (2017).
- [15] O. Bibikova, J. Haas, A. I. López-Lorente, A. Popov, M. Kinnunen, I. Meglinski, B. Mizaikoff, *Analyst.* **142**, 951 (2017).
- [16] V. Kaur, S. Singh, *Opt. Fiber Technol.* **48**, 159 (2019).
- [17] W. M. Mukhtar, R. M. Halim, K. A. Dasuki, A. R. A. Rashid, N. A. M. Taib, *Malaysian J. Fundam. Appl. Sci.* **26**, 619 (2017).
- [18] M. B. Hossain, M. S. Hossain, S. R. Islam, M. N. Sakib, K. Z. Islam, M. A. Hossain et al., *Results Phys.* **18**, 103281 (2020).
- [19] W. M. Mukhtar, R. M. Halim, K. A. Dasuki, A. R. A. Rashid, N. A. M. Taib, 2018 IEEE International Conference on Semiconductor Electronics (ICSE), 152 (2018).
- [20] A. M. Shrivastav, S. P. Usha, B. D. Gupta, *Biosens. Bioelectron.* **90**, 516 (2017).
- [21] W. M. Mukhtar, S. Shaari, P. S. Menon, *Adv. Sci. Lett.* **19**, 1412 (2013).
- [22] Yang, E. Kazuma, Y. Yokota, Y. Kim, *The Journal of Physical Chemistry C.* **122**, 16950 (2018).
- [23] W. M. Mukhtar, N. R. Ayob, R. M. Halim, N. D. Samsuri, N. F. Murat, A. R. A. Rashid, K. A. Dasuki, *J. Adv. Res. Mater. Sci.* **49**, 1 (2018).
- [24] R. A. Rather, S. Singh, B. Pal, *Sol. Energy Mater. Sol. Cells.* **160**, 463 (2017).
- [25] V. Semwal, B. D. Gupta, *Sens. Actuators B* **329**, 129062 (2021).
- [26] Shah, H. Reddy, N. Kinsey, V. M. Shalaeve, A. Boltasseva, *Adv. Opt. Mater.* **5**, 1700065 (2017).
- [27] A. H. El-Saeed, A. E. Khalil, M. F. O. Hameed, M. Y. Azab, S. S. A. Obayya, *Opt. Quantum Electron.* **51**, 1 (2019).
- [28] S. M. Edlou, J. C. Simons, G. A. Al-Jumaily, N. A. Raouf, *Optical Thin Films IV: New Developments. International Society for Optics and Photonics* 96 (1994).
- [29] N. F. Murat, W. M. Mukhtar, P. S. Menon, *Optoelectron. Adv. Mat.* **14**, 482 (2020).
- [30] G. V. Naik, J. Kim, A. Boltasseva. *Opt. Mater. Express* **1**, 1090 (2011).
- [31] N. F. Murat, W. M. Mukhtar, A. R. A. Rashid, K. A. Dasuki, A. A. R. A. Yusuf, 2016 IEEE International Conference on Semiconductor Electronics (ICSE), 244 (2016).
- [32] L. Novotny, B. Hecht, *Principles of Nano Optics*, United Kingdom: Cambridge University Press (2012).
- [33] D. Li, C. Weng, Y. Ruan, K. Li, G. Cai, C. Song, Q. Lin, *Sensors* **21**, 1003 (2021).
- [34] S. Magdi, M. A. Swillam, In *Physics, Simulation, and Photonic Engineering of Photovoltaic Devices VII*, **10527**, International Society for Optics and Photonics, 2018.

*Corresponding author: wmaisarah@usim.edu.my